

## RESEARCH ARTICLE

# Research on Reliability Growth of Chain Transmission System in Rapid Secure Device of Shipborne Helicopter

ZHUXIN ZHANG<sup>1,2</sup>, WEIJIAN LI<sup>1,3</sup>, DINGXUAN ZHAO<sup>1,3</sup>,  
BING WANG<sup>1,2</sup>, TAO NI<sup>1,2</sup>, AND TUO JIA<sup>1,2</sup>

<sup>1</sup>Hebei Key Laboratory of Special Delivery Equipment, Yanshan University, Qinhuangdao 066004, China

<sup>2</sup>School of Vehicle and Energy, Yanshan University, Qinhuangdao 066004, China

<sup>3</sup>School of Mechanical Engineering, Yanshan University, Qinhuangdao 066004, China

Corresponding author: Weijian Li (lwj-mh@stumail.ysu.edu.cn)


This work was supported in part by the Key Research and Development Program of Hebei Province under Grant 20353501D, Grant 21351802D, and Grant 22357601D.

**ABSTRACT** Aiming the chain transmission system in the rapid secure device (RSD) of shipborne helicopter, an individual fault was that the chain was broken, and then the system gave an alarm. According to the above question, the RSD reliability growth test bench was built to conduct a reliability growth test study on the chain transmission system in a single RSD test prototype. After the cause of the fault was found, a part of the chain in the test prototype was tested by the chain pulling test machine. According to the test results, the reliability optimization design of the chain transmission system was carried out, and the optimization design scheme was determined. A suitable reliability growth test plan for the chain transmission system was formulated using the Duane model analysis method. Through the reliability growth test, the Class B failure statistics of the chain transmission system were obtained, and then the reliability growth Duane model of the total test time of the chain transmission system was established. Using the army materiel systems analysis activity (AMSAA) model analysis method, the approximate unbiased estimation of the instantaneous mean time between failures (MTBF) of the chain transmission system was carried out, the trend test of the reliability growth of the chain transmission system was carried out, and the confidence interval of the instantaneous MTBF at the end of the test time was obtained to verify that the reliability optimization design meets the planning requirements and provide a reference for the reliability growth research of the whole RSD equipment.

**INDEX TERMS** Rapid secure device, chain transmission, reliability growth, Duane model, AMSAA model.

## I. INTRODUCTION

With the development of helicopters and surface ships, shipborne helicopters have become the conventional equipment of large surface ships. It not only makes up for the weaknesses of surface ships, such as poor maneuverability and narrow vision, but also performs tasks such as antisubmarine warfare, antiship warfare, electronic warfare, reconnaissance warning, and transportation [1]. At the same time as the development

The associate editor coordinating the review of this manuscript and approving it for publication was Agustín Leobardo Herrera-May .

of shipborne helicopters, how to ensure the safe take-off and landing, mooring, straightening, and towing of shipborne helicopters on deck has become an urgent problem for navies of various countries. Shipborne helicopter assisted landing and towing systems came into being [2]. The types of assisted landing and towing systems are as follows: Russian fishing net type assisted landing device and winch towing system. By adopting the method of arranging rough nylon nets on the deck apron, the shipborne helicopter is bound to the landing area of the deck, and then the shipborne helicopter is transported by the manual traction winch. The device is

now almost obsolete [3]. Harpoon-grille type assisted landing device and SAMACH towing system from DCNS, France. After the shipborne helicopter lands on the deck, the harpoon in its abdomen is inserted into the mesh steel grille and locked automatically. Then, the shipborne helicopter is drawn by the towing system composed of rail and tow tractor. This assisted landing device has a simple structure and is easy to load and unload, but it is only suitable for small shipborne helicopters [4], [5]. Canada Indal's E system (shipborne helicopter landing assistance and fixation system). Its working principle is that when the shipboard helicopter is hovering relative to the deck, the guide steel cable on its abdomen is connected and locked to the pull-down steel cable on the deck. The winch on the ship ensures that the shipborne helicopter can safely land on the deck by tightening or loosening the pull-down steel cable. However, only the Indian navy purchased two E2000 systems from 1977 to 1978 due to the system's long operating time, heavy weight, and the need for manpower to push the helicopter into/out of the hangar after mooring [6]. Recovery Assist Secure and Traverse (RAST) system from Indal, Canada [7]. This system was developed in 1974 based on the E system. It can complete operations such as pulling-down, mooring, adjusting the direction, and pulling in/out of the hangar for the shipborne helicopter. However, this system still requires the operators on deck to connect the guide steel rope to the pull-down steel rope, and the system track is too heavy. Indal and Gibbs & Cox from the United States developed a light track with half the weight of the prototype track in 1984, saving 60% of the cost and having a long life. It is called the second-generation RAST system [8]. Aircraft Ship Integrated Secure and Traverse System of Indal, Canada. This system consists of traction winch, rapid secure device (RSD), console, track, pilot visual cue system, and shipborne helicopter position detection system. The pilot can make an autonomous landing according to the visual cue system and the shipborne helicopter position detection system. During landing, the RSD always keeps track of the fixed rod on the belly of the shipborne helicopter. After the shipborne helicopter lands, the RSD captures the fixed rod longitudinally under the action of the traction winch, and the mechanical claw horizontally captures the fixed rod to complete the capture operation. The whole operation time is only 2 s, and it is the world's first set of fully automatic landing aid and traction system [9], [10].

At present, Chinese shipboard helicopters mainly have two types, Ka-28 and Z-9. The Ka-28 uses a Russian fishing net type assisted landing device. The use of this device causes the shipborne helicopter to have great requirements on the roll and pitch angles of the ship deck. The Z-9 uses a French harpoon-grille type assisted landing device, but this device is only suitable for a small shipborne helicopter with a self-weight of less than 5 t [11], [12], [13]. Therefore, the shipborne helicopter assisted landing device and towing system have become a short board that restricts the development of China's shipborne helicopter combat capability. RSD is an important part of the third-generation shipborne helicopter

assisted landing and towing system. It undertakes important tasks such as quickly capturing, mooring, straightening, and transferring shipborne helicopter to designated locations. The reliability of its operation is an important guarantee for the life safety of shipborne helicopter. Therefore, studying its reliability growth is necessary. The milestones in the development of reliability growth technology are the Duane empirical model summarized by J.T. Duane, an engineer of the General Electric Company of the United States, and the AMSAA model proposed by L.H. Crow of the U.S. Army Equipment System Analysis Center [14], [15], [16]. Chinese scholars have also conducted much research work in the field of reliability growth [17], [18], [19], [20], [21]. However, relatively minimal research has been performed on the reliability growth of marine-type equipment.

During the acceptance test of the RSD, the findings revealed that the chain transmission system driving the RSD mechanical claw had an alarm failure of the chain breaking. To realize the reliability growth of RSD, the failure analysis and reliability optimization design of the chain transmission system in the test prototype are carried out in this paper. Using the analysis methods of the Duane model and AMSAA model, the statistical estimation of the chain transmission system of the test prototype is carried out, which provides a theoretical basis for the subsequent RSD reliability growth.

## II. INTRODUCTION TO THE STRUCTURE AND WORKING PRINCIPLE OF RSD CHAIN TRANSMISSION SYSTEM

Figure 1 shows the schematic diagram of the internal structure of the RSD chain transmission system. This chain transmission system uses a pulley set structure that can increase the movement distance of the mechanical claw. When performing capture/release and straightening functions, the mechanical claw moves twice as far as the hydraulic cylinder piston rods. Figure 2 shows the physical diagram of RSD.

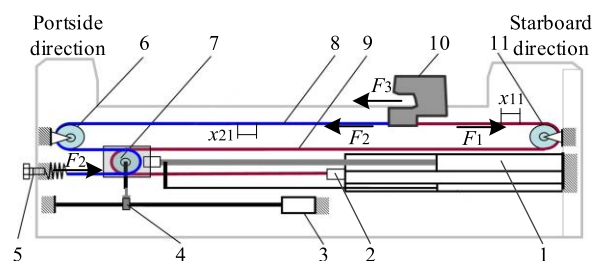


**FIGURE 1.** Schematic diagram of the internal structure of RSD chain transmission system: 1. Parallel connection single extension piston rod hydraulic cylinder, 2. Joint of pretensioned chain, 3. Magnetostrictive sensor body, 4. Magnetic ring, 5. Chain tensioning and breakage detection device, 6. Low fixed pulley, 7. Moving pulley, 8. Portside chain, 9. Starboard chain, 10. Mechanical claw, and 11. High fixed pulley.

Figure 3 shows a principle diagram of the hydraulic system of the RSD in capture/release and straightening conditions. The portside direction is the capture direction, and the starboard direction is the release direction. When the mechanical claw is in the capture/release condition, the

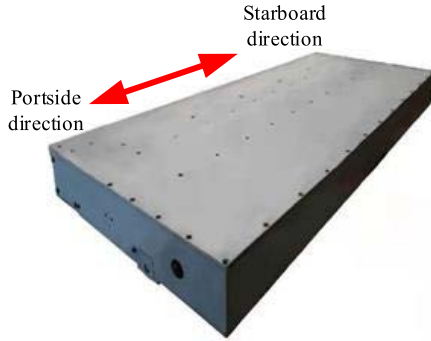


FIGURE 2. Physical diagram of RSD.

fine piston rod hydraulic cylinder in the parallel connection single extension piston rod hydraulic cylinder is in the high-speed, low-output force condition. The constant displacement pump and accumulator together supply pressure energy to the rod/ rodless chamber of the fine hydraulic cylinder. At this time, solenoid directional valve 9.6 is energized to open the external control hydraulic lock, so that the coarse hydraulic cylinder is in the floating state. When the mechanical claw is in the portside direction or starboard direction straightening condition, the parallel connection single extension piston rod hydraulic cylinder is low-speed, large-output force state. To ensure that the thrust forces of the parallel connection single extension piston rod hydraulic cylinder are approximately equal during the reciprocating motion. When the rodless chamber of the coarse hydraulic cylinder is supplied with oil and the piston rod is extended (i.e., the mechanical claw is straightened toward the starboard direction), solenoid directional valves 9.1 and 9.2 are de-energized and the fine hydraulic cylinder is in a floating state. When the mechanical claw is straightened to the portside direction, the piston rods are retracted, solenoid directional valve 9.1 is energized, and 9.2 is de-energized. The hydraulic oil acts together in the rod

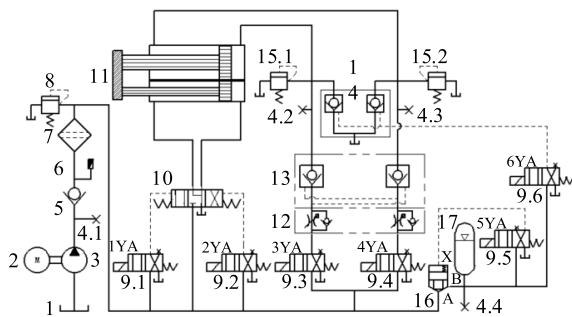


FIGURE 3. Principle diagram of the hydraulic system under RSD capture/release and straightening conditions: 1. Tank, 2. AC motor, 3. Constant displacement pump, 4. Pressure measuring joint, 5. Check valve, 6. Pressure sensor, 7. Fine filter, 8. Flood valve, 9. Two-position, four-way solenoid directional valve, 10. Three-position, four-way hydraulic control directional valve, 11. Parallel connection single extension piston rod hydraulic cylinder, 12. Double throttle check valve, 13. Internal control hydraulic lock, 14. External control hydraulic lock, 15. Relief valve, 16. Two-way cartridge valve, and 17. Accumulator.

chambers of the coarse hydraulic cylinder and fine hydraulic cylinder. The coarse cylinder circuit in the hydraulic system is equipped with two hydraulic locks, internal and external control. The combined action of the internally controlled hydraulic lock and externally controlled hydraulic lock can enable the parallel connection single extension piston rod hydraulic cylinder to withstand the reverse force of the external load, which ensures that the piston rods of the hydraulic cylinder are not pushed in the opposite direction.

### III. RELIABILITY OPTIMIZATION DESIGN OF RSD CHAIN TRANSMISSION SYSTEM

#### A. RELIABILITY TEST AND FAILURE PHENOMENON OF RSD CHAIN TRANSMISSION SYSTEM

Figure 4 shows the RSD reliability growth test bench. In the reliability test of the quick capture/release and straightening functions of the RSD, the RSD is first fixedly connected to the track slider. Under the action of the parallel connection double extension piston rod hydraulic cylinder, the RSD quickly approaches the simulated fixed rod under the belly of the shipboard helicopter along the deck simulation track at a speed of up to 1.2 m/s peak. Then, the simulated fixed rod triggers the rapid capture function of RSD. The simulated fixed rod can be anywhere in the RSD mechanical claw capture area of 2.0 m in the Y direction. After the mechanical claw captures the simulated fixed rod, when the RSD is in the mooring condition, the parallel connection single extension piston rod hydraulic cylinder is hydraulically locked up. The purpose is to ensure that the simulated fixed rod under the abdomen of the shipboard helicopter moored by the RSD in real sea conditions are not significantly displaced in the Y direction. When the simulated fixed rod loads a force of 50 kN on the mechanical claw toward the portside direction, the mechanical claw is hydraulically locked and the speed is 0. When the total reliability test is carried out for about 32 h, the RSD console shows a chain breakage alarm failure phenomenon, as shown in Figure 5.

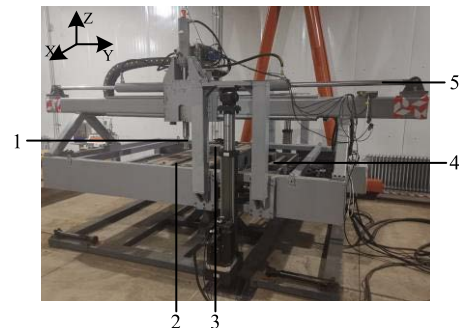


FIGURE 4. RSD reliability growth test bench: 1. Simulated fixed rod, 2. Simulated track, 3. Track slider, 4. X-direction parallel connection double extension piston rod hydraulic cylinder, and 5. Y-direction double extension piston rod hydraulic cylinder.



Chain break warning

FIGURE 5. RSD console chain breakage alarm interface.

**B. RSD CHAIN TRANSMISSION SYSTEM CHAIN BREAKAGE FAILURE CAUSE ANALYSIS**

The reliability growth test bench and RSD are always in working order while fault detection is being performed. The simulated fixed rod captured by the mechanical claw always outputs a simulated loading force of 50 kN in the portside direction. According to the console chain breakage alarm interface, the RSD is opened and the chain is not pulled off, but the chain breakage detection travel switch in the chain tensioning and breakage detection device is triggered.

Figures 1 and 6 show the working principle of the chain tensioning and breakage detection device designed in this paper: When the simulated fixed rod does not apply a simulated loading force to the mechanical claw, the direction of simulated loading force is portside. The pre tightening nut and the chain joint are connected by threads. The pre tightening nut is tightened to move the chain joint to the right, so that the starboard chain pre tightening force increases to  $F_1$ , and the portside chain pre tightening force increases to  $F_2$ . The equation is

$$F_2 = F_4 + F_5, \tag{1}$$

where  $F_4$  is the pre tightening body case to the pre tightening nut reverse force, and  $F_5$  is the tensioning spring to the pre tightening nut reverse force. The starboard chain elastic elongation value is  $x_{11}$ , and the portside chain elastic elongation value is  $x_{21}$ . When the simulated fixed rod starts to apply loading force to the mechanical claw, the loading force is toward the portside direction and increases gradually, and the starboard chain elastic elongation value increases to  $x_1$ . The equation is as follows:

$$x_1 = x_{11} + \Delta x_1, \tag{2}$$

where  $\Delta x_1$  is the change in the starboard chain elastic elongation value when the simulated fixed rod applies a loading force to the mechanical claw.

The increase of the starboard chain elastic elongation value directly leads to the decrease of the portside chain elastic elongation value, which causes the decrease of the portside chain pre tightening force  $F_2$ , until the reverse force  $F_4$  of the pre tightening body case toward the pre tightening nut is 0. The portside chain elastic elongation value is reduced by  $x_{21}$ , and the chain elastic elongation value caused by the pre tightening force exerted by the tensioning spring on the

portside chain is regarded as 0. As the loading force of the simulated fixed rod gradually increases, the change  $\Delta x_1$  of the starboard chain elastic elongation value also increases gradually. The tensioning spring pushes the pre tightening nut to the right to maintain the portside chain pre tightening force at  $F_5$ . When the change  $\Delta x_1$  of the starboard chain elastic elongation value is

$$\Delta x_1 = x_3 + x_4 + x_{21}, \tag{3}$$

the chain breakage detection travel switch is triggered by the Z-type baffle, and the console issues a chain breakage alarm failure.

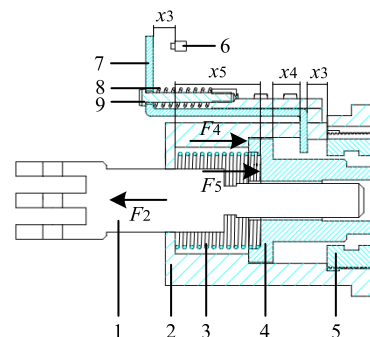


FIGURE 6. Chain tensioning and breakage detection device: 1. Chain joint, 2. Pre tightening body case, 3. Tensioning spring, 4. Pre tightening nut, 5. Welding block, 6. Chain breakage detection travel switch, 7. Z-type baffle, 8. Trigger spring, and 9. Screw.

**C. RELIABILITY OPTIMIZATION DESIGN OF RSD CHAIN TRANSMISSION SYSTEM**

First, for the above failure cause analysis of the chain transmission system’s chain breakage, a part of the RSD chain is subjected to a pulling force test using a chain pulling force test machine in this paper. Figure 7 shows the pitch of the chain is 25.4 mm, the combination of the number of chain plates is  $4 \times 4$ , and the number of chain links is 9.

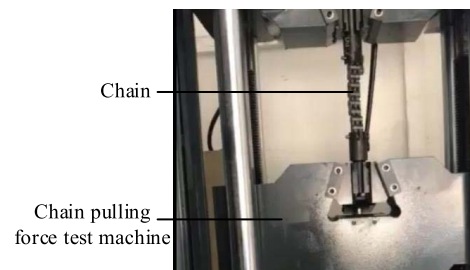


FIGURE 7. Chain pulling force test.

The test result of the chain pulling force test machine shows that the chain elastic elongation value is 6.978 mm when the pulling force reaches 132.31 kN. When the pulling force of the test machine is unloaded to 0 kN, the chain is plastically deformed, and the deformation amount is 1.971 mm. The lower yielding force of the chain is 67.62 kN. Figure 8 shows the chain pulling force test curves.

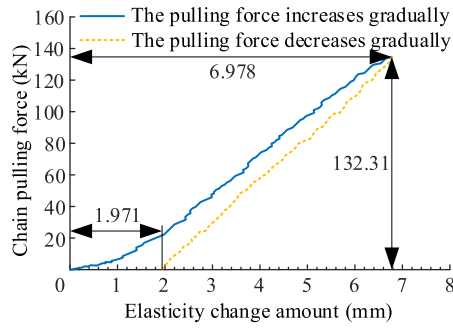


FIGURE 8. Chain pulling force test curves.

The number of links of the starboard chain in the RSD is 154, and the number of links of the portside chain is 103. Based on the above experimental results and after calculation, the parameters shown in Table 1 are obtained.  $F_1/F_2$  is the starboard/portside chain pre tightening force,  $\Delta x_1$  is the change in the starboard chain elastic elongation value, at which time the simulated fixed rod applies a simulated loading force to the mechanical claw that is hydraulically locked, the force magnitude is 50 kN, and the direction is portside.  $x_3 + x_4$  is the trigger stroke of the pre tightening nut in the chain tensioning and breakage detection device.

TABLE 1. Parameters table of chain pulling force and elastic elongation value.

$F_1/F_2$ (kN)	$x_{11}$ (mm)	$x_{21}$ (mm)	$\Delta x_1$ (mm)	$x_3+x_4$ (mm)
1	3.594	2.404	49.619	47.215
2	5.817	3.891	48.427	44.536
3	10.270	6.869	44.487	37.618
4	11.634	7.781	44.148	36.367
5	14.543	9.727	41.924	32.197
6	16.087	10.759	41.406	30.647
7	18.137	12.131	40.041	27.910
8	18.823	12.589	40.040	27.451
9	19.681	13.163	39.695	26.532
10	21.046	14.076	39.355	25.279
11	22.417	14.993	39.355	24.362
12	23.615	15.794	38.670	22.876
13	24.120	16.021	38.630	22.609
14	24.692	16.253	38.618	22.365
15	25.325	16.938	38.584	21.646
16	26.177	17.508	37.905	20.397
17	26.863	17.967	37.558	19.591

Before optimizing the design of the chain tensioning and breakage detection device, the trigger stroke  $x_3 + x_4$  of the pre tightening nut is 22 mm. At present, all technologies of RSD have been solidified. Based on the principle of small changes, the choices are two reliability optimized design schemes. Optimized design Scheme 1. According to Table 1, to prevent chain tensioning and breakage detection device from false alarm due to elastic deformation of chain under pulling force, when the mechanical claw is not loaded with simulated force, the starboard/portside chain pre tightening force  $F_1/F_2$  needs to be increased to at least 15 kN but not more than 17 kN to avoid the plastic deformation of the portside/starboard chain.

However, the magnitude and direction of the speed of the parallel connection double extension piston rod hydraulic cylinder are transmitted to the mechanical claw through the moving pulley set and the high/low fixed pulley. The increase in the starboard/portside chain pre tightening force  $F_1/F_2$  leads to an increase in the friction torque of the bearings in the moving pulley set and the high/low fixed pulley, further reducing the capture/release speed of the mechanical claw, as shown in Figures 1 and 3. Therefore, this optimized design scheme is not used in this paper.

Scheme 2 is to optimize the design of the chain tensioning and breakage detection device. As shown in Figure 6, The trigger stroke  $x_3 + x_4$  of the pre tightening nut is increased from 22 mm to 29 mm, the compression length  $x_5$  of the spring is changed from 33 mm to 40 mm, and the length of the spring under the condition of no external load is changed from 75 mm (the spring length at ultimate compression is 30 mm) to 90 mm (the spring length at ultimate compression is 38 mm). According to the parameters of chain pulling force and elastic elongation value in Table 1, the optimized chain tensioning and breakage detection device can not only reduce the starboard/portside chain pre tightening force  $F_1/F_2$  and increase the capture/release speed of the mechanical claw, but also leave a design margin for the trigger stroke of the pre tightening nut when applying the simulated force to the mechanical claw. The feasibility of the reliability optimization design scheme is verified.

#### IV. RELIABILITY GROWTH TEST ON THE CHAIN TRANSMISSION SYSTEM OF THE RSD TEST PROTOTYPE

After the RSD chain transmission system is optimally designed for reliability, a continuous, effective reliability test plan and steps are formulated to conduct a reliability growth test on the chain transmission system of the RSD test prototype.

##### A. RELIABILITY GROWTH TEST PLAN FOR THE CHAIN TRANSMISSION SYSTEM OF THE TEST PROTOTYPE

###### 1) DETERMINATION OF INITIAL MTBF

During the reliability test on the chain transmission system of the test prototype, when the total accumulated test time is about 32 h, an alarm of chain breakage occurs. Therefore, the reliability growth initial level  $\theta_1 = 32$  h of the chain transmission system of the test prototype is determined.

###### 2) ESTIMATION OF RELIABILITY GROWTH RATE

Extensive reliability growth test practice shows that for the newly developed complex products, the growth rate is usually 0.3–0.6 [22]. The reliability growth rate of aeroengines and hydraulic mechanical devices studied by American electrical engineer Duane is about 0.5 [23]. In this paper, through the failure cause analysis of chain breakage false alarm and the optimized design of chain tensioning and breakage detection device, the growth rate of the chain transmission system of the test prototype is predicted as  $m=0.5$ .

3) ESTIMATION OF TOTAL TEST TIME AND PLOTTING PLANNED GROWTH CURVES

According to the provisions of the research and development task book, the mean cycle between failures of RSD capture/release is not less than 200 times. In this reliability growth test, the RSD's operating time is calculated in 1 h (mooring time, straightening time, and towing time) for each capture and release action completed. Therefore, under the same stress conditions, the instantaneous mean time between failure (MTBF) of the chain transmission system of the test prototype must be increased to 6.25 times and more. The target value of reliability growth on chain transmission system of the test prototype is  $\theta_F = 200$  h in this test. Therefore, the total cumulative test time  $t_F$  when the target is reached is

$$t_F = t_I \left[ \frac{(1 - m) \theta_F}{\theta_I} \right]^{1/m} = 312.5, \quad (4)$$

according to the result of Equation (4), to make the instantaneous MTBF of chain transmission system reach 200 h, since the reliability growth initial level is 32 h, a reliability growth test of more than 280.5 h also needs to be carried out. After incorporating the first test section (0,  $t_I$ ] into the equation, the Duane model of the reliability growth plan is obtained based on the predicted parameters as

$$\theta_c(t) = \begin{cases} \theta_I = 32 & (0 < t \leq 32) \\ \theta_I \left(\frac{t}{t_I}\right)^m = 5.6569 \times t^{0.5} & (t > 32), \end{cases} \quad (5)$$

$$\theta(t) = \begin{cases} \theta_I = 32 & (0 < t \leq 32) \\ \theta_I \left(\frac{t}{t_I}\right)^m \frac{1}{1 - m} = 11.3137 \times t^{0.5} & (t > 32), \end{cases} \quad (6)$$

where  $\theta_c(t)$  is the cumulative MTBF of the chain transmission system of the test prototype at time  $t$ ,  $\theta(t)$  is the instantaneous MTBF of the chain transmission system of the test prototype at time  $t$ , and  $t_I$  is the cumulative test time of the first test section. According to the above reliability growth prediction model, its curves in the linear coordinate system and the logarithmic coordinate system are drawn, as shown in Figures 9 and 10.

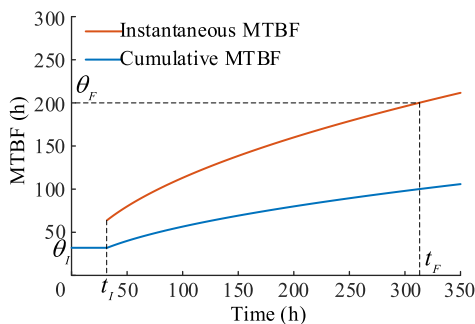


FIGURE 9. Planned growth curves in the linear coordinate system.

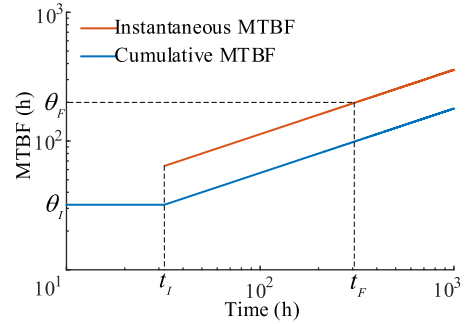


FIGURE 10. Planned growth curves in the logarithmic coordinate system.

B. RELIABILITY GROWTH TEST OF CHAIN TRANSMISSION SYSTEM OF TEST PROTOTYPE

1) PROCESS AND EFFECT OF RELIABILITY GROWTH TEST

According to the reliability growth plan and using the same load conditions and operating conditions as in the reliability test stage in an environment with an average temperature of about 25°C and humidity of about 40%, and the simulated force loading test on the mechanical claw by the simulated fixed rod, the accumulated time is about 200 h, the magnitude of the force is 50 kN, and the direction is portside. In the starboard direction, a further simulated force loading test with a cumulative time of about 200 h is performed. The total reliability growth test time is more than 400 h.

Combined with Figures 7 and 8, after the reliability optimization design, no chain false alarm failure occurs in the loading test over 200 h, which proves the feasibility of this reliability optimization design and provides the basic data for the next step of establishing the reliability growth model.

2) STATISTICS OF CLASS B FAILURES

Three Class B failures occur during the reliability growth test (Class B failures are those systematic failures that need to be corrected). After the correction, the reliability growth test is carried out again. The cumulative failure data of Class B failures for the total test time are shown in Table 2.

TABLE 2. Cumulative failure data table of total test time of chain transmission system in the test prototype after the optimized design.

Test time $t/h$	Number of failures $N(t)$	MTBF $t/N(t)$
32	1	32
102	2	51
198	3	66
400	3	133.33

V. RELIABILITY GROWTH MODEL OF CHAIN TRANSMISSION SYSTEM OF RSD TEST PROTOTYPE

A. SOLVING PARAMETERS OF DUANE MODEL BY THE LEAST SQUARE METHOD

According to the statistics of Class B failures, the failure statistics of the Duane model least square method for the

TABLE 3. Statistical data table of the failure of the least square method for the Duane model with complete data.

Order number	$N(t_j)$	$t_j/h$	$\ln t_j$	$(\ln t_j)^2$	$\theta_c(t_j)$	$\ln \theta_c(t_j)$	$\ln \theta_c(t_j) \ln t_j$
1	1	32	3.4657	12.0113	32	3.4657	12.0113
2	2	102	4.6250	21.3904	51	3.9318	18.1846
3	3	198	5.2883	27.9658	66	4.1897	22.1560
4	3	400	5.9915	35.8976	133.3300	4.8929	29.3154
Accumulation			19.7966	100.4001	299.3300	16.9062	84.8023

reliability growth test of the test prototype chain transmission system are obtained, as shown in Table 3.

Assuming that in the double logarithmic coordinate system, the difference between the reliability growth test data points of the test prototype chain transmission system and the reliability growth plan Duane model is  $\varepsilon_j$ , then the equation is

$$\sum_{j=1}^{n_1} \varepsilon_j^2 = \sum_{j=1}^{n_1} (\ln \theta_c(t_j) + \ln a - m \ln t_j)^2. \quad (7)$$

In the case where the residual sum of squares is the smallest, the following equations can be used.

$$\begin{aligned} \frac{\partial}{\partial \ln a} \sum_{j=1}^{n_1} \varepsilon_j^2 &= 0 \\ \Rightarrow \sum_{j=1}^{n_1} (\ln \theta_c(t_j) + \ln a - m \ln t_j) &= 0, \end{aligned} \quad (8)$$

$$\begin{aligned} \frac{\partial}{\partial m} \sum_{j=1}^{n_1} \varepsilon_j^2 &= 0 \\ \Rightarrow \sum_{j=1}^{n_1} (\ln \theta_c(t_j) + \ln a - m \ln t_j) \ln t_j &= 0, \end{aligned} \quad (9)$$

where  $n_1$  is the number of groups of the test data. According to Equations (8) and (9), the least square estimates of  $m$  and  $a$  are derived as

$$\hat{m} = \frac{n_1 \sum_{j=1}^{n_1} \ln \theta_c(t_j) \ln t_j - \left( \sum_{j=1}^{n_1} \ln \theta_c(t_j) \right) \cdot \left( \sum_{j=1}^{n_1} \ln t_j \right)}{n_1 \sum_{j=1}^{n_1} (\ln t_j)^2 - \left( \sum_{j=1}^{n_1} \ln t_j \right)^2}, \quad (10)$$

$$\hat{a} = \exp \left\{ \frac{1}{n_1} \left( \hat{m} \sum_{j=1}^{n_1} \ln t_j - \sum_{j=1}^{n_1} \ln \theta_c(t_j) \right) \right\}. \quad (11)$$

Thus, the Duane model for the reliability growth of the total test time of the chain transmission system of the test prototype is obtained as

$$\hat{\theta}(t_{n_1}) = \frac{t_{n_1}^{\hat{m}}}{\hat{a}(1 - \hat{m})} = 9.8594 \times t_{n_1}^{0.5375}, \quad (12)$$

where  $a$  is the scale parameter of the growth curves,  $m$  is the growth rate of the growth curves, and  $\hat{\theta}(t_{n_1})$  is the LSE of

instantaneous MTBF at  $t_{n_1}$  time. As a result, the reliability growth curves of the test prototype chain transmission system in the logarithmic coordinate system are shown in Figure 11.

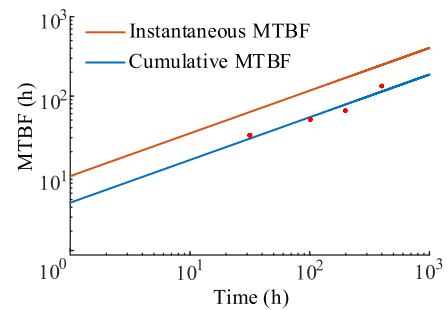


FIGURE 11. Duane curves of the test data.

### B. UNBIASED ESTIMATION OF AMSAA MODEL FOR CHAIN TRANSMISSION SYSTEM OF SINGLE TEST PROTOTYPE AT THE END OF THE TEST TIME

Based on the Duane model, the AMSAA model assumes that the number of failures  $N(t)$  of the repairable test prototype chain transmission system during the development period is an inhomogeneous Poisson process with mean function  $EN(t) = at^b$  and instantaneous intensity  $\lambda(t) = dEN(t)/dt = abt^{b-1}$ . Then, the MTBF after the chain transmission system of the repairable test prototype is developed to time  $T$  is

$$\theta(t) = \frac{1}{\lambda(t)} = \frac{T^{1-b}}{ab}, \quad (13)$$

where  $b$  is the shape parameter, and  $T$  is the total time of reliability growth. Based on the above assumptions and the likelihood function, the maximum likelihood estimate of the shape parameter is

$$\hat{b} = n_2 / \sum_{j=1}^{n_2} \ln \frac{T}{t_j} = 0.6528, \quad (14)$$

where  $n_2$  is the number of failures.  $0 < \hat{b} < 1$ , so failure time interval  $t_j - t_{j-1}$  ( $j = 1, 2, 3$ ) increases randomly as  $j$  increases, and instantaneous intensity  $\lambda(t)$  decreases strictly monotonically. Therefore, the chain transmission system of the test prototype is in the process of reliability growth.

From the unbiased estimation theorem in the AMSAA model, the following equation can be obtained,

$$E\left(\frac{n_2 - 1}{n_2} \hat{b} | N(T) = n_2\right) = b, \quad (15)$$

the unbiased estimate of shape parameter  $b$  obtained from Equation (15) is

$$\bar{b} = \frac{n_2 - 1}{n_2} \hat{b} = (n_2 - 1) \left/ \sum_{j=1}^{n_2} \frac{T}{t_j} \right. = 0.4352. \quad (16)$$

According to  $\bar{b}$ , when  $T = 400$  h, under the condition of complete data, the approximate unbiased estimate of the instantaneous MTBF of the test prototype chain transmission system is

$$\bar{\theta}(T) = T / (n_2 \bar{b}) = 306.3725. \quad (17)$$

**C. TREND TEST AT COMPLETE DATA UNDER AMSAA MODEL**

The reliability growth trend test is a statistical hypothesis test, which can make a probability judgment on whether the reliability of the test prototype chain transmission system has changed significantly during the test. The Laplace test method is used to test the reliability growth trend, and the specific process is as follows.

For the test data of the chain transmission system of a single test prototype at the end of the test time, the test statistic  $\mu$  in the case of  $M \geq 3$  is

$$\mu = \left( \frac{\sum_{j=1}^M t_j}{MT} - \frac{1}{2} \right) \sqrt{12M} = -1.3400, \quad (18)$$

where  $M$  is the goodness of fit test parameter, and  $M = n_2$ . The selection of the significance level  $\alpha$  is related to many factors. The smaller the value of  $\alpha$  is, the longer the required test time, but the conclusions drawn have a high degree of confidence, taking  $\alpha = 0.2$ , and the critical value of  $\mu$  is  $\mu_0 = 1.313$  by checking the table.

Comparing the test statistic  $\mu$  with the critical value  $\mu_0$ ,

$$\mu < -\mu_0. \quad (19)$$

Therefore, the chain transmission system of the test prototype has an evident reliability growth trend when the significance level is 0.2.

**D. GOODNESS OF FIT TEST AT COMPLETE DATA UNDER AMSAA MODEL**

To check whether the reliability growth data of the chain transmission system of the test prototype conforms to the AMSAA model, the Cramér–Von Mises test method is used to perform the goodness of fit test, and the specific test process is as follows.

The goodness of fit test statistic  $C^2(M)$  is calculated, and the equation is as follows:

$$C^2(M) = \frac{1}{12M} + \sum_{j=1}^M \left[ \left( \frac{t_j}{T} \right)^{\bar{b}} - \frac{2j-1}{2M} \right]^2 = 0.0676. \quad (20)$$

According to the significance level  $\alpha$  of the test and the value of the goodness of fit test parameter  $M$ , and after checking the table, the critical value  $C^2(M, \alpha)$  of  $C^2(M)$  is

$$C^2(M, \alpha) = C^2(3, 0.2) = 0.1210. \quad (21)$$

The calculated value of  $C^2(M)$  is compared with the critical value of  $C^2(M)$ , and the following equation is obtained,

$$C^2(M) = 0.0676 < C^2(M, \alpha) = 0.1210. \quad (22)$$

Comparing the calculated quantities in Equation (22) reveals that the calculated value of  $C^2(M)$  is less than the critical value  $C^2(M, \alpha)$ . The goodness of fit test does not reject the AMSAA model at a significance level of 0.2, and the AMSAA model can be used to fit the experimental data.

**E. SHAPE PARAMETER INTERVAL ESTIMATION AT COMPLETE DATA UNDER AMSAA MODEL**

The above verifies that the data of the chain transmission system of the test prototype can be statistically estimated using the AMSAA model. When the confidence level is  $\gamma = 0.8$ , the confidence interval  $[b_L, b_U]$  of the shape parameter  $b$  of the single test prototype chain transmission system at the end of the reliability growth time is

$$b_L = \frac{\bar{b}}{2(n_2 - 1)} \chi_{1-\frac{\gamma}{2}}^2(2n_2) = 0.2398, \quad (23)$$

$$b_U = \frac{\bar{b}}{2(n_2 - 1)} \chi_{\frac{1+\gamma}{2}}^2(2n_2) = 1.1582. \quad (24)$$

When the confidence level  $\gamma = 0.8$ , the unilateral upper confidence limit  $b_{U1}$  of the shape parameter  $b$  of the chain transmission system of the single test prototype is

$$b_{U1} = \frac{\bar{b}}{2(n_2 - 1)} \chi_{\gamma}^2(2n_2) = 0.9311. \quad (25)$$

$b_{U1} < 1$ , so the test prototype chain transmission system is in reliability growth at the time of the reliability growth test cutoff. The interval range of the instantaneous MTBF of the chain transmission system needs to be estimated.

**F. INSTANTANEOUS MTBF INTERVAL ESTIMATION AT COMPLETE DATA UNDER AMSAA MODEL**

The confidence level  $\gamma = 0.8$ , and the number of failures  $n_2 = 3$ . According to the AMSAA model time ending interval estimation coefficient  $[\pi_1, \pi_2]$  table,  $\pi_1 = 0.222$ , and  $\pi_2 = 4.217$ .



For the reliability growth test under the end of time condition, the non-randomized confidence interval  $[\theta_L, \theta_U]$  of the MTBF at  $T = 400$  h is obtained as

$$\theta_L = \pi_1 \bar{\theta}(T) = 68.0147, \quad (26)$$

$$\theta_U = \pi_2 \bar{\theta}(T) = 1291.9728. \quad (27)$$

Thus, the confidence interval of the instantaneous MTBF of the chain transmission system of the test prototype is obtained as [68.0147, 1291.9728]. After correcting the data for the approximate unbiased estimation of the instantaneous MTBF, the correction result is obtained as

$$[\bar{\theta}_L, \bar{\theta}_U] = [306.3725, 1291.9728]. \quad (28)$$

## VI. CONCLUSION

In this paper, for the chain transmission system driving RSD mechanical claw, the fault of chain breaking false alarm occurs, and the reliability growth test bench of RSD is built. The reliability test of the chain transmission system of a single test prototype is carried out. Failure analysis is performed for the recurring failure phenomenon. Two reliability optimization design schemes are proposed, reliability growth tests are conducted, the following conclusions are obtained.

(1) The test data for the reliability growth of the chain transmission system of a single test prototype are obtained. According to the reliability test, the initial MTBF of the chain transmission system of the test prototype is determined as 32 h. A reliability growth plan with a reliability growth rate of 0.5, a reliability growth target value of 200 h, and a total reliability growth test time of 280.5 h is developed. The reliability growth test is carried out on the chain transmission system of the optimized test prototype, and three failures occur. After taking the reliability growth measures, the reliability growth test is continued, and the time ends at 400 h.

(2) Adopting Option 2 is correct and feasible for the reliability optimization design of the chain transmission system of the test prototype. After the chain transmission system of the test prototype is designed optimally, the instantaneous MTBF of its reliability growth test increases to more than 200 h. Based on Class B failure statistics, using the least square method, in the double logarithmic coordinate system, the reliability growth Duane model of the chain transmission system of the test prototype is obtained as  $\hat{\theta}(t_n) = 9.8594 \times t_n^{0.5375}$ .

(3) The reliability growth test of the optimally designed test prototype chain transmission system can be statistically inferred by the AMSAA model. In the case of a single test prototype chain transmission system test time cutoff at complete data, the following conclusions are obtained. The approximate unbiased estimate of the instantaneous MTBF at  $T = 400$  h is 306.3725 h. The interval estimate of the shape parameter  $b$  under the AMSAA model is [0.2398, 0.9311]. The instantaneous MTBF interval at the confidence level of 0.8 is estimated as [306.3725, 1291.9728]. The chain transmission system of the test prototype is still in the process of reliability growth at the end of the reliability

growth test, and the instantaneous MTBF can reach about 1292.9728 h. This paper provides a theoretical basis for the long-term reliable operation of RSD.

## ACKNOWLEDGMENT

Author Contributions: Zhuxin Zhang: Designed the system structure, analyzed the working principle of the system, designed the reliability growth test bench, and analyzed the cause of the failure; Weijian Li: Analyzed the cause of the failure, conducted and analyzed the reliability growth test, and wrote the article; Dingxuan Zhao: Helped to calculate the Duane model and perform statistical estimation using the AMSAA model; Bing Wang: Contributed to the experiments; Tao Ni: Checked the relevant calculation for the model and interpretation of the conclusion; and Tuo Jia: Contributed to the background.

## REFERENCES

- [1] W. Feng and C. Lv, "Impact of shipborne helicopter technology development on mission capability," *Helicopter Technique*, vol. 49, no. 2, pp. 64–67, Jun. 2020.
- [2] H. Yu, "Integrated logistic support of shipboard helicopter," *Helicopter Technique*, vol. 33, no. 4, pp. 38–42, Dec. 2004.
- [3] H. Wu, D. Tan, Q. Li, and S. He, "Development trend analysis of a technical system of foreign helicopter assist secure and traverse equipment," *Ship Eng.*, vol. 43, no. S2, pp. 49–52, Nov. 2021.
- [4] B. Sun, "Assisted landing device for shipboard helicopter," *Modern Weaponry*, vol. 18, no. 10, pp. 37–38, Oct. 1995.
- [5] X. Liang, "Analysis on dynamic characteristics of shipborne helicopter assisted deck-landing," M.S. thesis, Dept. Aerospace Eng., Nanjing Univ. Aeronaut. Astronaut., Nanjing, China, 2018.
- [6] Z. Yu, "Development of shipboard helicopter pulling and lowering device," *Helicopter Technique*, vol. 27, no. 4, pp. 40–43, Nov. 1998.
- [7] W. G. Stewart and A. Baekken, "Helicopter rapid securing device," U.S. Patent 3 303 807, Feb. 14, 1967.
- [8] X. Chang, "Landing aid device of a shipborne helicopter," *Ordnance Knowl.*, vol. 35, no. 10, pp. 78–81, Oct. 2013.
- [9] B. Fu, "Take-off and landing and landing aid of a shipboard helicopter," *Flight Test*, vol. 14, no. 2, pp. 65–68 and 81, 1990.
- [10] H. Wu, D. Tan, Q. Li, S. He, and X. Zhang, "Comparative analysis on the comprehensive performance of foreign shipborne helicopter assist secure and traverse equipment," *Ship Sci. Technol.*, vol. 43, no. 23, pp. 185–189, Dec. 2021.
- [11] T. Wei and Y. Tian, "Development and application of Chinese navy's Zhi-9 shipborne helicopter," *Shipborne Weapons*, vol. 16, no. 5, pp. 48–61, May 2008.
- [12] M. Zhang, "Harpoon-grid type vs. haul-down type helicopter landing aid system comparison," *NAAS Inertial Technol.*, vol. 29, no. 7, pp. 69–78, Jul. 2015.
- [13] Y. Xu, "The strategy of shipboard helicopter safe path planning," M.S. thesis, Dept. Aerospace Eng., Nanjing Univ. Aeronaut. Astronaut., Nanjing, China, 2020.
- [14] J. T. Duane, "Learning curve approach to reliability monitoring," *IEEE Trans. Aerosp.*, vol. AS-2, no. 2, pp. 563–566, Apr. 1964.
- [15] L. H. Crow, "Confidence interval procedures for the Weibull process with applications to reliability growth," *Technometrics*, vol. 24, no. 1, pp. 67–72, 1982.
- [16] L. H. Crow and A. P. Basu, "Reliability growth estimation with missing data. II," in *Proc. Annu. Rel. Maintainability Symp.*, Los Angeles, CA, USA, Jan. 1988, pp. 476–483.
- [17] Q. Ru, "Research on reliability growth of FAST hydraulic actuator hydraulic integrated pipeline system," M.S. thesis, Dept. Mech. Eng., Yanshan Univ., Qinhuangdao, China, 2019.
- [18] D. Pan, "Research on the application of reliability growth test of a vehicle based on the Duane mode," *Auto Mobile Sci. Technol.*, vol. 48, no. 5, pp. 17–24, Sep. 2020.
- [19] X. Guo, Z. Zhang, X. He, and J. Li, "Preliminary study on reliability growth test of iodine pneumatic valve in COIL," *High Power Laser Part. Beams*, vol. 28, no. 10, pp. 7–12, Aug. 2016.

- [20] Z. Wang, Z. Wang, H. He, K. Guo, J. Wang, and L. Zhao, "Study on reliability growth of turbine of turbocharger for vehicle applications with over-speed failure mode," *China Mech. Eng.*, vol. 27, no. 3, pp. 408–412, Jan. 2016.
- [21] Z. Fan and D. Xie, "Research on reliability growth of the gear box based on the cold-extruded strengthening technology," *Vehicle Power Technol.*, vol. 40, no. 3, pp. 14–17 and 29, Sep. 2018.
- [22] W. Mei, *Reliability Growth Test*, 1st ed. Beijing, China: National Defense Industry Press, 2002, pp. 23–101.
- [23] W. An and J. Hu, *Research on Reliability Growth Test Method*, 1st ed. Harbin, China: Harbin Engineering Univ. Press, 1996, pp. 20–62.



**ZHUXIN ZHANG** received the B.S. degree in fluid power transmission and control from the Northeastern University of Technology, Shenyang, China, in 1986, the M.S. degree in fluid power transmission and control from the Northeastern University, Shenyang, in 1996, and the Ph.D. degree in mechanical and electronic engineering from Jilin University, Changchun, China, in 2009. He is currently a Professor and the Ph.D. Supervisor with the Hebei Key Laboratory of Special

Delivery Equipment, Yanshan University. He has conducted several projects from the National Key Technology Research and Development Program and the Key Research and Development Program of Province. His current research interests include equipment reliability, engineering robot technology, electrohydraulic control technology, and research on mechanism and robot technology.



**WEIJIAN LI** received the B.S. degree in fluid power transmission and control from the School of Liren, Yanshan University, Qinhuangdao, China, in 2015, and the M.S. degree in fluid power transmission and control from Yanshan University, in 2018, where he is currently pursuing the Ph.D. degree with the Hebei Key Laboratory of Special Delivery Equipment. His current research interests include reliability research of equipment and fluid power transmission and control.



**DINGXUAN ZHAO** received the B.S. degree in mechanical engineering from the Xi'an University of Architecture and Technology, Xi'an, China, in 1985, and the M.S. and Ph.D. degrees in engineering machinery from the Jilin University of Technology, Changchun, China, in 1988 and 1992, respectively. He is currently a Professor and the Ph.D. Supervisor with the Hebei Key Laboratory of Special Delivery Equipment, Yanshan University, where he is the President. He has conducted

several projects from the National Key Technology Research and Development Program and the Key Research and Development Program of Province. His current research interests include dynamics and simulation of complex mechanical systems, automatic transmission and energy saving control of construction vehicles, pavement spectrum acquisition and reproduction technology, and engineering robot technology.



**BING WANG** received the B.S. degree from the Henan Institute of Engineering, Zhengzhou, China, in 2017. He is currently pursuing the M.S. degree with the Hebei Key Laboratory of Special Delivery Equipment, Yanshan University. His current research interests include advanced design technology and reliability research of equipment.



**TAO NI** received the B.S. degree in mechanical and electronic engineering from Shandong University Technology, Zibo, China, in 2000, and the M.S. and Ph.D. degrees in mechanical and electronic engineering from Jilin University, Changchun, China, in 2003 and 2006, respectively. He is currently a Professor and the Ph.D. Supervisor with the School of Vehicle and Energy, Yanshan University. His current research interests include intelligent mobile robot technology, virtual reality, and simulation technology.



**TUO JIA** received the M.S. degree in mechanical and electronic engineering and the Ph.D. degree in mechanical design and theory from Jilin University, Changchun, China, in 2013 and 2020, respectively. He is currently a Lecturer with the School of Vehicle and Energy, Yanshan University. His current research interests include engineering robot technology and research on the mechanism and robot technology.

...